Liquid Crystals
Publication details, including instructions for authors and subscription information:
http://www.informaworld.com/smpp/title~content=t713926090

The dynamics of the CH_3CN molecule in the isotropic phase and in a nematic solution

D. Imbardelli[a]; G. Chidichimo[a]; P. Bucci[a]
[a] Chemistry Department, Univerity of Calabria, Arcavacata di Rende, CS, Italy

To cite this Article Imbardelli, D. , Chidichimo, G. and Bucci, P.(1990) 'The dynamics of the CH_3CN molecule in the isotropic phase and in a nematic solution', Liquid Crystals, 7: 6, 895 — 909
To link to this Article: DOI: 10.1080/02678299008033847
URL: http://dx.doi.org/10.1080/02678299008033847

LIQUID CRYSTALS, 1990, VOL. 7, NO. 6, 895–909

The dynamics of the CH_3CN molecule in the isotropic phase and in a nematic solution

by D. IMBARDELLI, G. CHIDICHIMO and P. BUCCI
Chemistry Department, Univerity of Calabria, 87030 Arcavacata di Rende (CS), Italy

(*Received 20 November 1989; accepted 16 December 1989*)

NMR lineshape studies of acetonitrile in the isotropic and the liquid-crystalline nematic phase of PCH have been performed. The scalar relaxation of the second kind due to the presence of the ^{14}N quadrupolar nucleus has been confirmed as the most important relaxation mechanism for this molecule in both the isotropic and the anisotropic phase. It has been found largely responsible for the selective broadening on ^{13}C and ^{1}H transitions. A minor contribution arising from intramolecular dipolar relaxation mechanism has also been investigated. Linewidth analysis of the NMR spectra allowed us to determine the quadrupolar relaxation time T_{1N} of the ^{14}N nucleus. This is connected to the correlation time for rotational diffusion perpendicular to the molecular symmetry axis. A possible explanation of a residual selective broadeining which effects the ^{13}C and ^{1}H NMR transitions and is not taken into account by this mechanism, is also given.

1. Introduction

The nuclear magnetic relaxation of acetonitrile has been extensively studied in the past. Among the studies performed on CH_3CN in the iostropic phase [1–7] the work of Bopp [7] on deuterium relaxation should be noted. Several relaxation experiments have also been performed on acetontrile dissolved in liquid-crystalline solution. [8–13]. Longitudinal relaxation of ^{13}C and ^{14}N nuclei has been investigated by Lopez Cardozo *et al.* [9]. Selective inversion recovery experiments and cyano ^{13}C linewidth measurements performed on acetonitrile in Phase V allowed Luyten *et al.* [8] to obtain the longitudinal relaxation of ^{1}H, ^{13}C and ^{14}N. Grant *et al.* [10] have measured T_1 for ^{1}H and ^{13}C nuclei by inversion recovery experiments; they used the perdeuteriated nematic phases (EBBA-d_{23}) for the proton relaxation study in order to minimize the intermolecular dipolar interactions, while undeuteriated EBBA was used as the solvent when ^{13}C relaxation was studied. Jaffe *et al.* measured the deuteron relaxation of acetonitrile-d_{23} dissolved in the nematic of Phase V by using multiple quantum spin echo linewidth measurements [12] in conjunction with inversion recovery experiments. The same authors also studied the frequency and temperature dependence of spin lattice relaxation and determined the relaxation rate of quadrupolar order by Jeener–Broekaert pulse sequences [13].

Our study is concerned with the transverse relaxation of the CH_3CN molecule in isotropic and anisotropic media, using linewidth and lineshape analysis of ^{1}H and ^{13}C NMR transitions. The aim of our work is to show that this approach, which has been recently adopted for successful studies of molecular dynamics in anisotropic media [17, 20, 21] can yield the same information usually obtained by more complex experimental techniques which use ^{13}C enriched samples. It must be emphasized that

0267–8292/90 $3.00

for single transitions the relaxation analysis can be given in terms of the widths, while for degenerate transitions the lineshape must be considered. The results of such an investigation is a unique set of parameters, which give the best fit of linewidth, for a single transition, and lineshape, for degenerate transitions. In fact, in the latter case overlapping transitions have not, in principle, the same width and as a result the half width at half height of the resultant lines becomes meaningless.

The following procedure has been used to account for the observed linewidths of ^{1}H and ^{13}C NMR transitions. First, the widest ^{13}C lines, coming from the cyano group carbon, have been reproduced in terms of the scalar relaxation mechanism due to the coupling of this ^{13}C with the ^{14}N quadrupolar nucleus. The contribution of such a scalar relaxation on this particular transition is in fact large such that other mechanisms give only secondary effects which are lost in the experimental error. The equation of motion of the statistical operator for the CH_3CN spin system has been solved in the Liouville space [14, 24]. The contribution of the scalar relaxation to the linewidth has been expressed in terms of: (i) direct and indirect dipolar couplings between the ^{14}N nucleus and the other nuclei, which were determined by diagonalizing the static hamiltonian; (ii) the quadrupolar relaxation time T_{1N} of the N nucleus. The values of T_{1N} is greater in the isotropic phase than in the nematic phase, confirming that the reorientational process affecting the quadrupolar relaxation is slower in the liquid-crystalline solvent.

Once the T_{1N} quadrupolar relaxation time is determined by reproducing the ^{13}CN linewidth, the minor effect of the scalar relaxation on the ^{1}H and methyl ^{13}C nuclei were calculated. T_{1N} has then been used to determine the value of $\tau_\perp$, which is connected to the rotational diffusion tensor component perpendicular to the CH–CH_3 symmetry axis ($D_\perp$). This dynamical parameter has been adopted to estimate the contribution of the intramolecular dipolar relaxation mechanism to the linewidth in the framework of the rotational diffusion model [20–23].

As we shall show, these mechanisms give contributions which can be estimated by using only one independent parameter (T_{1N}), but do not completely account for the observed linewidths. We have proposed a possible explanation for the residual broadening in terms of magnetic field inhomogeneity and a random fluctuating field [18, 19]. This last mechanism describes both the intermolecular dipolar interactions which act upon the proton magnetization and the spin-rotation interactions which affect the ^{13}C nuclei.

2. Experimental

The anisotropic sample was prepared by mixing 5 per cent wt of CH_3CN with PCH Licrystal (Merck, Darmstad), while the isotropic sample was pure liquid CH_3CN. In order to avoid paramagnetic relaxation by oxygen both samples were sealed in NMR Wilmad Imperial tubes under a nitrogen atmosphere after degasing. NMR spectra were taken at room temperature, with a Bruker WM-300 spectrometer; the nematic samples remained in the magnet for almost 24 h in order to achieve good thermal equilibrium and uniform orientation of the director.

For the nematic solutions, the measurement of proton transitions required only 24 scans, while the observation of ^{13}C magnetization was more difficult: transitions due to the methyl carbon were recorded after 250 scans, while those arising from the cyano ^{13}C, being very broad, needed 10000 scans. We have in fact observed that using 10000 scans (8 hours recording time) to record the $^{13}CH_3$ transitions a 4 Hz

broadening, corresponding to an error of 100 per cent, is introduced. Such an extra broadening, probably due to the orientational order fluctuations, caused by temperature variations, can be assumed to be absent when the recording time is reduced to 10 min (250 scans). We observed reproducible values of the linewidths when reducing the number of scans and repeating the experiments several times. On the other hand, the order fluctuations give an extra broadening of less than 4 Hz on the ^{13}CN transitions, since the dipolar coupling (absolute value) of this nucleus with protons is four times smaller than the dipolar coupling measured for the methyl carbon. Thus the effect of the extra broadening introduced by long accumulation times can be neglected for the ^{13}CN nucleus, which has very broad natural linewidths due to the coupling with the fast relaxing quadrupolar ^{14}N nucleus. In fact it is easy to verify that in our case the broadening introduced by the scalar relaxation mechanism is practically unaffected by small variations of the orientational order. In the isotropic phase the measurement of ^{13}C spectrum required 16 scans.

3. Theory

The theoretical treatment of the relaxation mechanism affecting the NMR spectra of the CH_3CN molecule in both isotropic and anisotropic solutions is illustrated in the following paragraphs.

3.1. *Scalar relaxation*

A simple model to determine the relaxation due to the coupling of the ^{14}N quadrupolar nucleus with the other nuclei has been given by Abragam [16]. On the other hand, the theory developed by Pyper to treat the scalar relaxation in isotropic media [14, 15] is more general. Extension of this theory to anisotropic solutions has been made by inserting in the coupling hamiltonian the dirct dipolar couplings which arise from the partial orientation of the solute molecule in the liquid-crystalline solvent [17]. Solving the equation of motion for the reduced density matrix for the spin system according to the method of Pyper [14], $1/T_2$ of a non degenerate spin 1/2 transition $i - j$ is found to be

$$\tfrac{1}{2}\Delta\nu = \frac{1}{2\pi}\frac{1}{T_2} = \frac{R_{ijij}}{2\pi} = \frac{1}{2\pi}\left\{-2J_{iijj}(0) + \sum_c J_{cjcj}(\omega_{jc}) + \sum_c J_{cici}(\omega_{ci})\right\}. \quad (1)$$

The same result could also have been obtained by applying Abragam's theory. The spectral densities J_{cjcj} when the perturbation $\mathscr{H}_1$ (expressed in rad^{-1}) is truncated to its pseudosecular term

$$\mathscr{H}_1 = \sum_n 2\pi(J_{nx} + 2D_{nx})I_{zn}I_{zx}, \quad (2)$$

are obtained as

$$\begin{aligned} J_{cjcj}(\omega_{cj}) &= \sum_{\vartheta,\phi}\frac{4\pi^2}{L}\int_0^\infty \exp(i\omega_{\vartheta\phi}\tau)\exp(i\omega_{cj}\tau)\exp(-\tau/T_{1N})d\tau \\ &\quad\times\sum_{n,m}(J_{nx}+2D_{nx})(J_{mx}+2D_{mx})\langle\vartheta|I_{zx}|\phi\rangle\langle\phi|I_{zx}|\vartheta\rangle\langle c|I_{zn}|j\rangle\langle j|I_{zm}|c\rangle, \\ &= \delta_{cj}\frac{4\pi^2}{3}\sum_{\phi=1,-1}\sum_{n<m}(J_{nx}+2D_{nx})(J_{mx}+2D_{mx})[\langle\phi|I_{zx}|\phi\rangle]^2 \\ &\quad\times\langle c|I_{zn}|j\rangle\langle j|I_{zm}|c\rangle T_{1N}, \end{aligned} \quad (3)$$

where L is the number of eigenstates $|\vartheta\rangle$ and $|\phi\rangle$ of the ^{14}N nucleus, connected by a transition which occurs at frequency $\omega_{\vartheta\phi}$, and ω_{cj} is the frequency of the transition between the energy levels c and j of the spin 1/2 nuclei.

3.2. *Intramolecular dipolar interactions*

The hamiltonian which describes the intramolecular dipolar interactions can be written [16] as

$$\mathscr{H}_D(t) = \sum_{\substack{l,m \\ i<j}} (-1)^m F_m^{(i,j)} D_{lm}^2(\Omega) A_l^{(i,j)}, \tag{4}$$

where $F_{-m}^{(i,j)}$ is the second rank tensor, expressed in the molecular frame, describing the geometry of the dipolar interaction; $A_l^{(ij)}$ is the spin tensor expressed in the laboratory frame; $D_{lm}^2(\Omega)$ is the Wigner rotation matrix which describes the reorientation of the molecular frame with respect to the laboratory frame. The contribution of the intramolecular dipolar interactions to the linewidths can be calculated following the theoretical procedure suggested in [20, 21]. The equation for the rotational diffusion motion in the presence of an orienting potential is solved according to the methodologic appraoch of Nordio and coworkers [22, 23]. The spectra densities which enter in the Redfield matrix element are given by

$$J_{lm}(\omega) = \sum_{\substack{i<j \\ p<q}} F_{-m}^{(i,j)} F_m^{(p,q)} (\langle\alpha|A_{\pm l}^{(i,j)}|\beta\rangle\langle\beta'|A_{\mp l}^{(p,q)}|\alpha'\rangle K_{lm}(\omega_{\alpha\beta})$$

$$- \delta_{\alpha'\beta'} \sum_{\gamma} \langle\gamma|A_{\pm l}^{(i,j)}|\beta\rangle\langle\alpha|A_{\mp}^{(p,q)}|\gamma\rangle K_{lm}(\omega_{\gamma\beta}) - \delta_{\alpha\beta} \sum_{\gamma} \langle\gamma|A_{\pm l}^{(i,j)}|\alpha'\rangle\langle\beta'|A_{\mp l}^{(p,q)}|\gamma\rangle K_{lm}(\omega_{\gamma\beta'}), \tag{5}$$

where $K_{lm}(\omega)$ is the generic spectral density of the Wigner rotation matrices. It is a function of the eigenvalues and the eigenvectors of the rotational diffusion operator defined in the linear space of Wigner functions

$$K_{lm}(\omega) = \sum_K a_{klm} \frac{D_\perp \alpha_{lm}^k}{(D_\perp \alpha_{lm}^k)^2 + \omega^2}; \tag{6}$$

here $D_\perp$ is the rotational diffusion tensor element describing a rotation around an axis perpendicular to the molecular symmetry axis α_{lm}^k, which is the kth eigenvalue, can be determined for particular indices l, m, and depends on the strength of the ordering potential in the nematic solution as well as on the ratio of $D_\parallel$ and $D_\perp$, the rotational diffusion tensor element connectd to the rotation around the symmetry axis of the molecule. The coefficient a_{klm} is a linear combination of the eigenvectors of the rotational diffusion operator calculated according to the model proposed by Nordio *et al.* [22, 23].

4. Results

The first step of our linewidth analysis was the determination of the time independent spectral parameters both in the isotropic and the nematic phase. The direct dipolar couplings $D_{^{13}C-H}$ were obtained from the ^{13}C satellites in the amplified ^1H NMR spectra, since the low signal-to-noise ratio of the ^{13}C spectra did not allow sufficiently precise determination of these constants. According to figure 1, where the molecule fixed axes are shown, only the element S_{zz} of the saupe ordering matrix is needed to describe the molecular order. This element has been calculated using

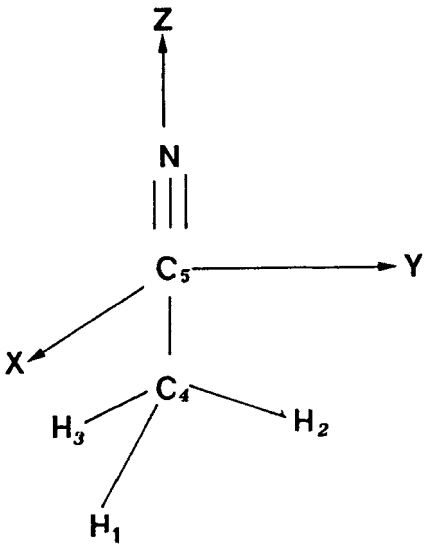

Figure 1. Nuclear notation and molecular axis system for the CH_3CN molecule.

standard geometrical information [25, 26] from [27];

$$D_{ij} = -(\gamma_i\gamma_j h/8\pi^2 r_{ij}^3)[S_{zz}(3\cos^2\vartheta - 1)], \quad (7)$$

where $\mathbf{r}_{ij}$ is the internuclear vector between nuclei i and j, and ϑ_{rz} is the angle between this vector and the z axis. A value for S_{zz} of 0·1136 was obtained.

The orientational parameter S_{zz} and the geometrical data given in table 1 were than used to evaluate the coupling constants $D_{^{14}N-H}$ and $D_{^{14}N-^{13}C}$, which are required to determine the contributions of the scalar relaxation of the second kind. The scalar couplings $J_{^{14}N-H}$ and $J_{^{13}C-^{14}N}$, which are also needed for the calculation of the scalar relaxation contribution, were obtained by scaling the values reported by other authors [28, 30] for the ^{15}N-labelled acetonitrile (scaling factor $\gamma_{^{14}N}/\gamma_{^{15}N} = -0{\cdot}713$). All these spectral parameters are reported in table 1 according to the numbering scheme given in figure 1.

Table 1. Indirect J_{ij} and direct D_{ij} dipolar couplings, internuclear distances R_{ij} [27, 30], order parameter S_{zz} in nematic solution for acetonitrile.

Pairs of nuclei	J_{ij}/Hz	D_{ij}/Hz	r_{ij}/Å
H–H	–	1106·973 ± ·05†	1·8308
$^{13}C_4$–H	136·23 + ·05	753·400 ± ·08†	1·1282
$^{13}C_5$–H	10·00 + ·05	−221·400 ± ·85†	2·1334
^{14}N–H	1·2836‡	−25·740 ± ·28§	3·1677
^{14}N–$^{13}C_4$	−2·1394‡	−14·186 ± ·15§	2·5917
^{14}N–$^{13}C_5$	12·4797‡	−169·797 ± 1·85§	1·1330
		$S_{zz} = 0{\cdot}11360 \pm {\cdot}00150$	

‡ Spectral parameters measured directly.

‡ Indirect dipolar couplings evaluated on the basis of the results reported by other authors [26, 28].

§ D_{zz} couplings evaluated by using equation (10).

Table 2. Anisotropic CH_3CN. Separate contributions to the linewidths represented in figures 2, 3 and 4, in terms arising from different relaxation mechanisms. The second column reports the intensity of the transitions. $\Delta\nu_{(T_{1N})}$ is the contribution due to the scalar relaxation mechanism; $\Delta\nu_{(1D)}$ is the contribution due to the intramolecular dipolar relaxation; $\Delta\nu_{(EXP)}$ is the experimental linewidths; $\Delta\nu_{(RES)}$ is the residual linewidths = $\Delta\nu_{(EXP)} - \Delta\nu_{T_{1N}} - \Delta\nu_{(RFMF)}$ is the sum of the magnetic field inhomogeneity and the random fluctuating field broadening.

Nucleus	Transition	Intensity	$\Delta\nu_{(T_{1N})}$/Hz	$\Delta\nu_{(1D)}$/Hz	$\Delta\nu_{(EXP)}$/Hz	$\Delta\nu_{(RES)}$/Hz	$\Delta\nu_{(RFMF)}$/Hz
	1	3·0	3·0	1·4	6·6 + 0·3	2·2 + 0·3	2·2
	2	1·0	3·0	0·0	Overlapping	.	1·4
Prot.	3	1·0	3·0	0·0	transitions	++	1·4
H_1	4	4·0	3·0	0·6			2·6
H_2							
H_3	5	3·0	3·0	1·4	6·6 ± 0·3	2·2 + 0·3	2·2
	6	1·0	1·2	1·0	3·6 ± 0·3	1·4 + 0·3	1·4
C_4†	7	1·0	1·2	0·8	Overlapping		2·4
	8	1·0	1·2	0·2	transitions	‡	0·9
	9	1·0	1·2	0·2			0·9
	10	1·0	136·5	0·4	140 ± 10·6	2·6 + 10·6	1·4
C_5†	11	1·0	136·5	0·4	Overlapping		2·4
	12	1·0	136·5	0·0	transitions	‡	0·9
	13	1·0	136·5	0·0			0·9

† For the carbon nuclei, only the transitions of the low field half of the spectra are reported since the symmetrical high field transitions are equivalent.

‡ These three transitions overlap and the linewidth of each one is not connected by analytical expression to the linewidth of the resulting line. Then for these overlapping transitions only the comparison between the resulting theoretical lineshapes and the experimental lines can be made $\Delta\nu_{(RES)}$ cannot be calculated.

A further step in our study has been the linewidth analysis of the ^1H and ^{13}C NMR spectra. The cyano ^{13}C transitions were observed to be broader than the methyl ^{13}C transitions, both in the isotropic and anisotropic phase. Since the cyano ^{13}C nucleus is directly bound to the ^{14}N, it was suggested that, as in the case of partially oriented pyridine [17], the most relevant contributiom to the linewidth comes from the scalar relaxation. According to equations (1)–(3) the broadening due to this a relaxation mechanism allows us to determine the value of T_{1N}, this is found to be $1{\cdot}43 \times 10^{-4}$ s. On the other hand this dynamical parameter is connected to $\tau_\perp$ by

$$\frac{1}{T_{1N}} = \tfrac{3}{2}\pi^2(e^2Qq_{zz}/h)^2\tau_\perp, \tag{8}$$

which is written on the assumption that for symmetry reasons the rotation around the molecular symmetry axis has no influence. Using this equation with T_{1N} of $1{\cdot}43 \times 10^{-4}$ s and a quadrupolar coupling constant of 3·6 MHz [29], a value of $\tau_\perp = 3{\cdot}64 \times 10^{-11}$ s was obtained. This value has been used in equation (6) in order to obtain the broadening due to the intramolecular dipolar interactions.

Table 2 illustrates that both the scalar and the intramolecular dipolar mechanisms are selective, that is to say, they broaden each line in a different way. The fit of the

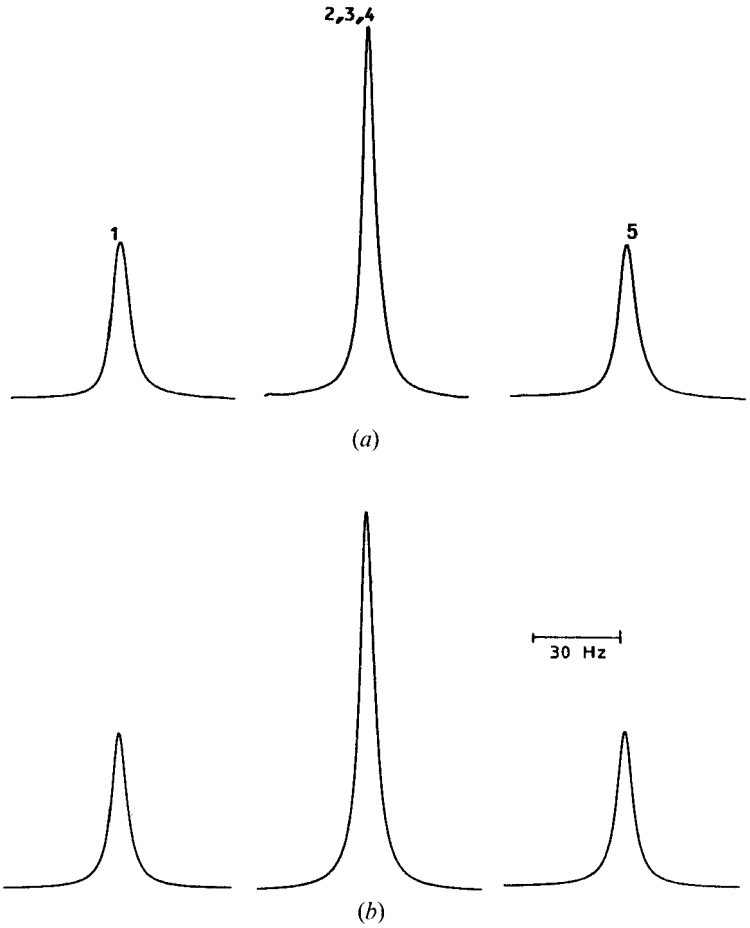

Figure 2. CH_3CN in the liquid-crystalline phase. Experimental (*a*) and calculated (*b*) linewidths obtained for the ^1H NMR transitions.

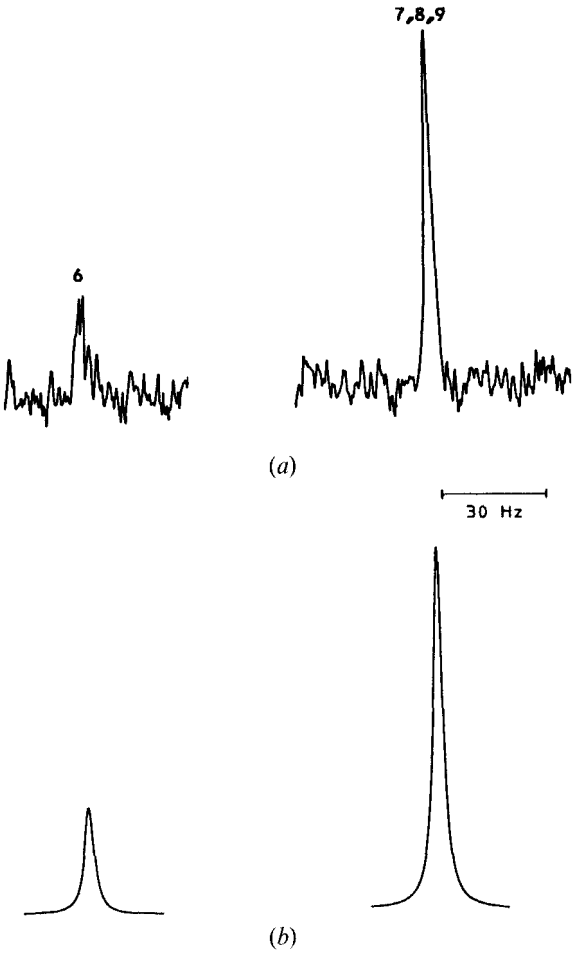

Figure 3. CH_3CN in the liquid-crystalline phase. Experimental (*a*) and calculated (*b*) line-widths obtained for two transitions of the methyl ^{13}C nucleus.

^{13}C linewidths belonging to the cyano group could be only given in terms of the scalar mechanism, while for the proton and the methyl group ^{13}C transitions, this scalar relaxation is not so important and gives differential contributions which are comparable to the dipolar broadening. Moreover the theoretical linewidths obtained as the sum of the scalar and the intramolecular contributions do not completely reproduce the experimental transitions. The difference between the experimental and the theoretical linewidths is not the same for all the transitions, as shown in table 2. An attempt has been made to explain this residual differential broadening in terms of other relaxation mechanisms, such as the magnetic field inhomogeneity (this would give a constant contribution to all the line widths) and the random fluctuating field which would relax each transition in a selective way. The random fluctuating field is a simplified model often used to have a simple picture of more complex relaxation mechanisms; when applied to proton transitions it describes the relaxation from intermolecular dipolar interactions, and for ^{13}C line-widths describes the relaxation from spin rotation interactions. The contribute of the random fluctuating field has been calculated according to [19]; the value used for $f(\omega)$ in our case is $5{\cdot}6 \times 10^{10}$ s.

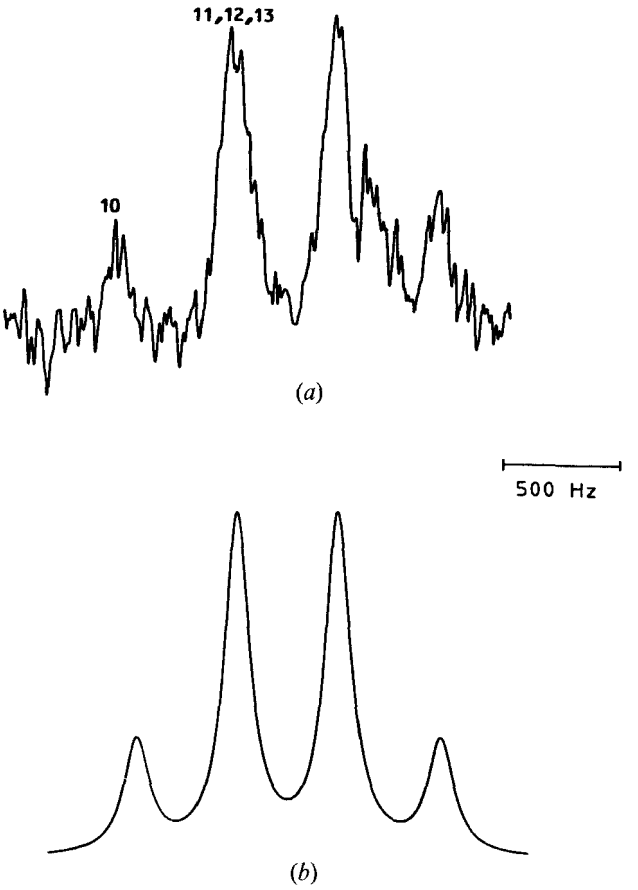

Figure 4. CH_3CN in the liquid-crystalline phase. Experimental (*a*) and calculated (*b*) linewidths obtained for the cyano ^{13}C NMR transitions.

The magnetic field inhomogeneity $\Delta\nu_0$ adopted is 1 Hz for the protons and 0·25 for the carbons.

In table 2, the theoretical contributions of these two mechanisms $\Delta\nu_{(RFMF)}$ are compared with the discrepancies observed between the experimental data and the linewidth calculated when considering only the scalar and intramolecular dipolar mechanisms $\Delta\nu_{(T_{1N})} + \Delta\nu_{(ID)}$. As can be seen the agreement is very good, in spite of the small number of adjustable parameters (actually, only one was used to calculate both the spin rotational interaction, which affects the ^{13}C transitions, and the intermolecular dipolar contribution to the ^1H linewidths). Obviously, such a coincidence can be only accidental and probably due to the fact that the contribution to the experimental linewidth which exceeds the sum of scalar and intramolecular dipolar broadening is not very discrimininating with respect to the many relaxing mechanisms that can be taken into account. We report further calculations only for the sake of completness.

In figures 2 (*a*), 3 (*a*) and 4 (*a*) the transitions of the experimental spectra obtained from CH_3CN in nematic solution are suitably expanded, in order to enable a comparison with the calculated lines in figures 2 (*b*), 3 (*b*) and 4 (*b*). Figure 2 illustrates the fit of the proton transitions. Figure 3 shows the fit of the methyl ^{13}C transitions

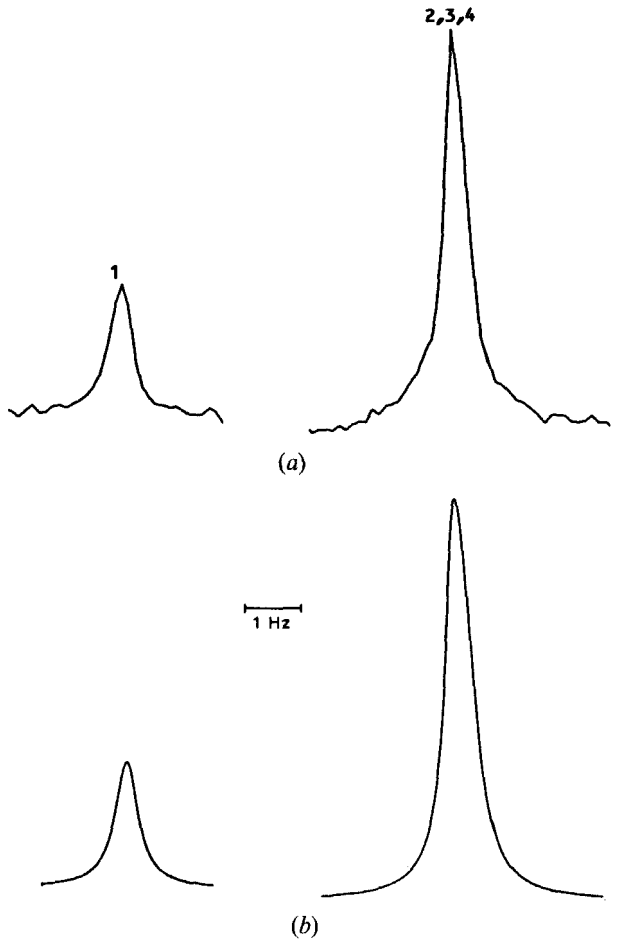

Figure 5. CH_3CN in the isotropic phase. Experimental (*a*) and calculated (*b*) linewidths obtained for the two methyl ^{13}C NMR low field transitions.

(only two transitions are shown: the other two, belonging to the high field half of the spectrum, are symmetric with respect to the lines reported). Figure 4 illustrates the experimental and the theoretical lines obtained for the cyano ^{13}C nucleus. In this case the signal-to-noise ratio is very poor because of the very broad lines. This effect does not prevent a reliable determination of T_{1N}, since the scalar relaxation contribution to the linewidth is two orders of magnitude larger than the experimental error which affects the measurements:

The fit of the lineshape of the ^{13}C NMR spectra obtained in the isotropic phase (see figures 5 and 6) has been performed with the same relaxation mechanisms which have been observed in the liquid-crystalline phase. As in the anisotropic solution the broadening of the cyano ^{13}C lines is larger than that observed in the methyl carbon transitions. In this case, the contribution of the scalar relaxation is due to the modulation (via quadrupolar relaxation) of the indirect dipolar interactions between the ^{14}N and the cyano ^{13}C nuclei, and consequently is less effective than in the nematic solution where the direct dipolar interactions are also present.

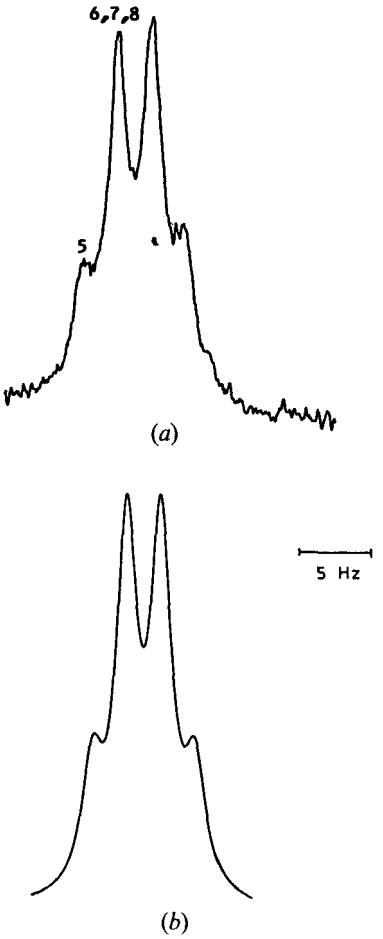

Figure 6. CH_3CN in the isotropic phase. Experimental (*a*) and calculated (*b*) linewidths obtained for the cyano ^{13}C NMR transitions.

The best fit parameters are

(*a*) $T_{1N} = 5{\cdot}41 \times 10^{-3}$ s (which gives a value for $\tau_\perp$ of $1{\cdot}02 \times 10^{-12}$ s through equation (8));
(*b*) $f(\omega)$ [19] $= 1 \times 10^{-10}$ s;
(*c*) $\Delta\nu_0 = 0{\cdot}08$ Hz.

The different behaviour of the methyl and the cyano ^{13}C transitions with respect to the scalar relaxation is presented in table 3. The contributions of the spin-rotation relaxation mechanisms to the linewidths are comparable for both the carbon nuclei. Since the broadening due to the intramolecular dipolar relaxation calculated for the value of $\tau_\perp$ derived from T_{1N} ($\tau_\perp = 1{\cdot}02 \times 10^{-12}$ s) is about 10^{-2} Hz, it has not been considered in table 3.

Table 4 has been included in order to have a quantitative picture of the lineshape analysis performed for both isotropic and anisotropic phases. The linewidth was measured only for single transitions. Obviously for the degenerate transitions the comparison between the experiemental and theoretical lines can only be made in terms

Table 3. Isotropic CH_3CN. Separate contributions to the linewidths of figures 5 and 6, from different relaxation mechanisms. The notation of the various contributions is equivalent to that adopted in table 2.

Nucleus	Transition	Intensity	$\Delta\nu_{(T_{1N})}$/Hz	$\Delta\nu_{(EXP)}$/Hz	$\Delta\nu_{(RES)}$/Hz	$\Delta\nu_{(RFMF)}$/Hz
	1	1·0	0·21	0·49 ± 0·05	0·20 ± ·05	0·24
	2	1·0	0·21	Overlapping		0·17
C_4	3	1·0	0·21	transitions		0·17
	4	1·0	0·21			0·39
	5	1·0	7·06	Overlapping		0·24
C_5	6	1·0	7·06	transitions		0·17
	7	1·0	7·06			0·17
	8	1·00	7·06			0·39

Table 4. Comparison between experimental and calculated linewidths. σ is the lineshape standard deviation (see text). The error reported are extremes on the basis of the variation observed by repeating the linewidth measurements several times.

	Line	$\Delta\nu_{exp.}$/Hz	$\Delta\nu_{theor.}$/Hz	σ/Hz
Anisotropic phase	1	6·6 ± 0·3	6·6	0·053
	2, 3, 4	Overlapping transitions		0·036
	6	3·6 ± 0·3	3·6	0·066
	7, 8, 9	Overlapping transitions		0·045
	10	140·0 ± 10·6	136·3	0·298
	11, 12, 13	Overlapping transitions		0·090
Isotropic phase	1	0·49 ± 0·05	0·45	0·054
	2, 3, 4	Overlapping transitions		0·035
	5, 6, 7, 8	Overlapped transitions		0·041

of a lineshape analysis. The standard deviation reported in table 4 has been estimated for all the lines from

$$\sigma = \left\{ \sum_{k=1}^{N} [(I(\omega_k)_{exp} - I(\omega_k)_{theor})^2/N]^{1/2} \right\}, \quad (9)$$

where $I(\omega_k)_{exp}$ and $I(\omega_k)_{theor}$ are the normalized $(I(\omega_k)/I(\omega_k)_{max})$ intensities of the transitions as measured at frequencies ω_k (ten different values of $I(\omega_k)$ have been used; $N = 10$). As can be seen, the precision of our analysis is about 5 per cent. However, for transition number 10 the error is much larger because of the poor signal-to-noise ratio.

5. Conclusion

The study of NMR transverse relaxation of the CH_3CN molecule provides an interesting example of comparing the relative importance of different relaxation mechanisms. The first observation to be emphasized is that the linewidth of the cyano ^{13}C transition is determined by the scalar relaxation due to the presence of the ^{14}N nucleus. The effect of this relaxation mechanism decreases for the methyl ^{13}C transitions and becomes comparable to the influence of the spin-rotation relaxation. When a comparison of the results obtained in the isotropic and anisotropic phases is taken into account, our study shows that the quadrupolar relaxation time T_{1N} of the ^{14}N nucleus is 40 times faster in the liquid-crystalline solution than in the isotropic solution. This strong variation can be explained in terms of modifications of the rotational diffusion around the molecular axes when going from the isotropic medium to the liquid-crystalline environment.

The results of our linewidth analysis have been compared to those obtained in earlier work. The authors of [7] who used Phase V instead of PCH as the solvent, reported a linewidth for the methyl ^{13}C lines of 1 Hz; in our case the linewidth is about 4 Hz. This would indicate a connection between the particular nematic phase used as solvent and the speed of the molecular motion which determine the effectiveness of the relaxation mechanism involved. This has already been confirmed for partially ordered pyridine [17]. In fact, the line broadening produced by the scalar relaxation due to the ^{14}N nucleus has been found to be strongly dependent on the chemical nature of the particular nematic solvent used.

Table 5. Comparison between our results for the correlation time of the rotational diffusion motion $\tau_\perp$ and the results of earlier studies.

$\tau_\perp/10^{-12}$ s	Isotropic phase	Nematic phase
(†)	1·02	36·4 (T = 20°C)
[1]	0·98	
[2]	1·10	
[7]	1·23	
[9]		72·0 (T = 22°C)
[8]		68·0 (T = 13°C)
[10]		26·4 (T = 38°C)
[13]		43·0 (T = 21°C)

† Results obtained in the present study.

Apart from these considerations, the order of magnitude of our dynamical parameters is in agreement with previous determinations. As an example, table 5 compares the values of $\tau_\perp$ obtained in our study for the isotropic and anisotropic phase and the values obtained by other authors. As we can see, the results obtained for the isotropic phase are in a very good agreement with earlier work. The difference which have been found for the anisotropic phase can be ascribed to the different temperatures and nematic solvents used in the experiments.

References

[1] Moniz, W. B., and Gutowsky, H. S., 1963, *J. chem. Phys.*, **38**, 1155.
[2] Woessner, D. E., Snowden, B. S., Jr., and Strom, E. T., 1968, *Molec. Phys.*, **14**, 265.
[3] Bull, T. E., and Jonas, J., 1975, *J. chem. Phys.*, **62**, 222.
[4] Leipert, T. K., Noggle, J. H., and Gillen, K. T., 1974, *J. magn. Reson.*, **13**, 158.
[5] Versmond, H., 1978, *Ber. Bunsenges. phys. Chem.*, **82**, 451.
[6] Tiffon, B., Ancian, B., and Dubois, J. E., 1981, *J. chem. Phys.*, **74**, 6981.
[7] Bopp, T. T., 1967, *J. chem. Phys.*, **47**, 3621.
[8] Luyten, P. R., Bulthuis, J., Bovee, W. M. M. J., and Plomp, L., 1982, *J. chem. Phys.*, **78**, 1712.
[9] Cardozo, H. L., Bulthuis, J., and McLean, C., 1979, *J. magn. Reson.*, **33**, 27.
[10] Black, E. P., Bernassau, J. M., Mayne, C. L., and Grant, D. M., 1982, *J. chem. Phys.*, **76**, 265.
[11] Courtieu, J., Lai, N. T., Mayne, C. L., Bernassau, J. M., and Grant, D. M., 1982, *J. chem. Phys.*, **76**, 259.
[12] (*a*) Jaffe, D., Vold, R. R., and Vold, R. L., 1982, *J. magn. Reson.*, **46**, 475; (*b*) 1982, *Ibid.*, **46**, 496.
[13] (*a*) Jaffe, D., Vold, R. L., and Vold, R. R., 1983, *J. chem. Phys.*, **78**, 4852.
[14] (*a*) Pyper, N. C., 1971, *Molec. Phys.*, **20**, 449. (*b*) Pyper, N. C., 1971, *Molec. Phys.*, **20**, 470.
[15] Pyper, N. C., 1971, *Molec. Phys.*, **21**, 1.
[16] Abragam, A., 1961, in *The Principles of Nuclear Magnetism* (Clarendon Press), chap. VIII.
[17] Imbardelli, D., Chidichimo, G., and Longeri, M., 1987, *Chem. Phys. Lett.*, **135**, 319.
[18] Lynden Bell, R. M., 1967, *Prog. NMR Spectrosc.*, **2**, 16.
[19] Sharma, B. B., Chidichimo, G., Saupe, A., Chang, M., and Brown, G. H., 1982, *J. magn. Reson.*, **49**, 287.
[20] Chidichimo, G., Imbardelli, D., Longeri, M., and Saupe, A., 1986, *Advanced Magnetic Resonance Techniques in Systems of High Molecular Complexity*, edited by I. Bertini and H. B. Gray (Birkhauser Verlag).
[21] Imbardelli, D., and Chidichimo, G., 1987, *Chem. Phys. Lett.*, **134**, 96.
[22] Nordio, P. L., Rigatti, G., and Segre, U., 1972, *J. chem. Phys.*, **56**, 2117; 1973, *Molec. Phys.*, **25**, 129.

[23] NORDIO, P. L., and SEGRE, U., 1979, *The Molecular Physics of Liquid Crystals*, edited by G. R. Luckhurst and G. W. Gray (Academic Press).
[24] JEENER, J., 1982, *Adv. Magn. Reson. Spectrosc.*, **10**, 1.
[25] ENGLERT, G., and SAUPE, A., 1969, *Molec Crystals*, **8**, 233.
[26] MCFARLANE, W., 1966, *Molec. Phys.*, **10**, 603.
[27] EMSLEY, J. W., and LINDON, J. C., 1975, *NMR Spectroscopy Using Liquid Crystal Solvents* (Pergamon Press).
[28] AXENROD, T., 1973, *Nitrogen NMR*, edited by M. Witanowski and G. A. Webb (Plenum Press).
[29] GERACE, M. J., and FUNG, B. M., 1970, *J. chem. Phys.*, **53**, 984.
[30] COSTAIN, C. C., 1958, *J. chem. Phys.*, **29**, 864.